Available online at www.sciencedirect.com
SCIENCE DIRECT
ELSEVIER
Palaeogeography, Palaeoclimatology, Palaeoecology 231 (2006) 199–214
PALAEO
www.elsevier.com/locate/palaeo

Late Quaternary glacial marine to marine sedimentation in the Pennell Trough (Ross Sea, Antarctica)

C. Salvi [a,*], M. Busetti [b], L. Marinoni [c], A. Brambati [a]

[a] *Dipartimento di Scienze Geologiche, Ambientali e Marine, Università di Trieste, Via E. Weiss 2, 34127 Trieste, Italy*
[b] *Istituto Nazionale di Oceanografia e di Geofisica Sperimentale, Borgo Grotta Gigante 42/c, 34010 Sgonico, Trieste, Italy*
[c] *Dipartimento di Scienze della Terra, Università di Pavia, Via Ferrata 1, 27100 Pavia, Italy*

Received 26 December 2004; accepted 8 July 2005

Abstract

Late Pleistocene and Holocene palaeoenvironmental changes were studied in four gravity cores up to 7.8 m long from the Pennell Trough, a NW–SE-trending basin 160 km long and 60 km wide in the central Ross Sea, Antarctica, with depths occasionally greater than 600 m. Differences in environments and depositional processes during the last glacial and postglacial epochs were investigated using X-rays and volume magnetic susceptibility (VMS). Further analyses included bulk and clay mineral composition, micropalaeontological studies (both benthic and planktic foraminifera) and radiometric dating. We compare our sedimentological, geochemical (organic carbon and nitrogen content), and geotechnical (shear strength and water content) results to those on cores previously taken from the region. These analyses suggest that prior to the Last Glacial Maximum (LGM), a glacial marine diamicton (<37,000 yr BP uncorrected age) was deposited across the basin from beneath an expanded Ross ice shelf that was grounded on the basin flanks. Sediment gravity flow deposits (27,000–21,000 yr BP uncorrected ages) that overlie the diamicton in the deepest part of the southernmost area of the basin are interpreted to have been deposited during the Last Glacial Maximum (~18,000 yr BP) as remobilized subglacial diamicton from the flanks of the basin, initiated by the movement of grounded ice. These sediments are followed by a period of non-deposition caused by basin starvation after retreat of the grounding line of Ross Sea ice far to the south. As a consequence, terrigenous supply was limited, and the persistence of floating shelf ice followed by multi-year sea-ice coverage inhibited the biogenic activity. During the Holocene, as climate became warmer, summer open-sea conditions began to dominate, leading to the deposition of a thin diatomaceous mud/ooze draping the basin.

Keywords: Ross Sea; Pennell Trough; Late Pleistocene and Holocene; Palaeoenvironmental changes; Glacial marine sedimentation

1. Introduction

The Ross Sea continental shelf morphology is characterized by deep troughs (up to 1500 m deep) and banks (Davey, 1995, 2004), shaped by advance and retreat of ice streams flowing from Transantarctic Mountains and Marie Byrd Land (Hughes, 1977; Anderson et al., 1992; Shipp et al., 1999). Sediment filling these troughs records the advance and retreat of grounded and floating ice during the last glacial–interglacial cycle, and their study contributes to our knowledge of palaeoenvironmental and palaeoclimatic variations across the entire region. Each basin, according to its distance from the grounding line, morphology, depth, etc., has a separate depositional history, but while Drygalski and JOIDES Basins have extensive

* Corresponding author. Tel.: +39 040 5582027; fax: +39 040 5582048.
E-mail address: salvi@univ.trieste.it (C. Salvi).

0031-0182/$ - see front matter © 2005 Elsevier B.V. All rights reserved.
doi:10.1016/j.palaeo.2005.07.034

databases (Licht et al., 1996, 1999; Domack et al., 1999; Brambati et al., 1997, 2002; Finocchiaro et al., 2000; Giglio et al., 2000), the Pennell Trough has more limited information (Hilfinger et al., 1995; Domack et al., 1999; Howat and Domack, 2003).

The Pennell Trough, located in the central Ross Sea with a north–west/south–east elongation (Fig. 1), is about 160 km long and 60 km wide, with depths occasionally greater than 600 m. It is separated by a sill from the continental slope to the north, and is flanked by a gently sloping Pennell Bank to the northeast and a steeper Ross Bank to the southwest. Both banks rise to depths of ~250 m.

The most widespread Plio-Quaternary sediment in the Ross Sea continental shelf is diamicton of glacial origin. Distinguishing subglacial from glacial marine diamicton is fundamental to the recognition of grounded ice on the continental shelf, and hence the maximum extent of glaciation. Anderson and Molnia (1989) recognized diamicton to be of subglacial origin when shear strength exceeds 2.5 kg/cm^2 (Anderson et al., 1992). In the western Ross Sea continental shelf, Licht et al. (1996) distinguished a glacial marine diamicton from a subglacial diamicton, being present North and South of the 74° S, respectively, on the basis of: 1) higher total organic carbon content; 2) presence of tephra layers and stratification; 3) higher diatom content and foraminifera abundance; 4) higher sand content, and 5) radiocarbon dates in chronological order downcore. Domack et al. (1999) hypothesized that in some cases the subglacial diamicton was initially deposited in a marine setting and remolded by the most recent glacial advance within the Ross Sea.

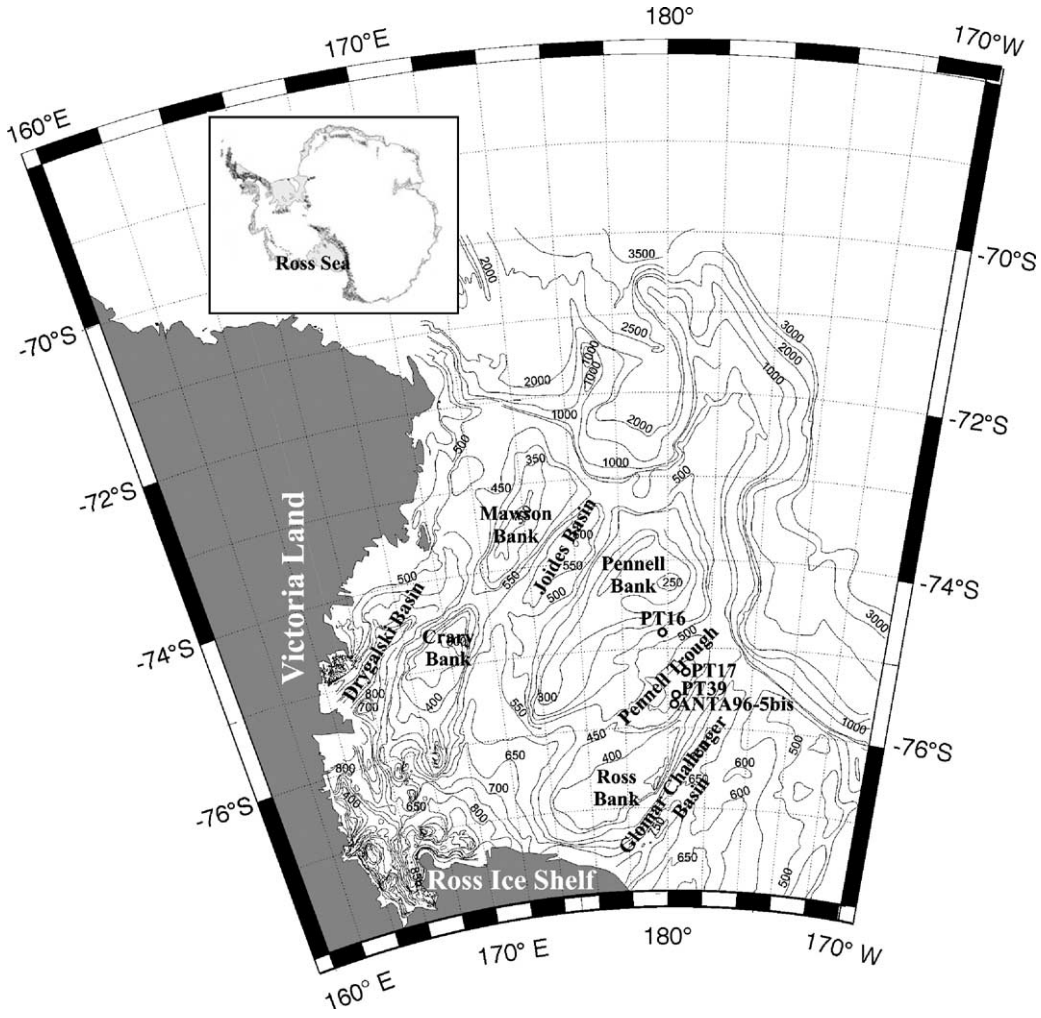

Fig. 1. Bathymetry of the Ross Sea (modified from Davey, 2004).

The results of Licht et al. (1996), which indicated that the grounding line for Ross sea ice ran approximately east–west at 74° S during the Last Glacial Maximum (LGM), has been refined by Shipp et al. (1999) and Howat and Domack (2003). Acoustic facies analysis suggests that grounded ice extended northward of 74° S in correspondence of the Mawson and Pennell Banks, but remained behind the southern flanks of JOIDES Basin and Pennell Trough. They identified the maximum extension of LGM ice at the southern end of the Pennell Trough, where subglacial deposits belonging to a series of back-stepping moraine ridges were found. The absence of grounded ice in the JOIDES Basin has been confirmed by subsequent sedimentological studies by Brambati et al. (2002).

A biogenic siliceous mud/ooze indicative of open marine conditions lies above the diamicton. In cores from the outer continental shelf, Licht et al. (1996) identified a hiatus from about 20,000 to 7000 yr BP located between diamicton and the biogenic siliceous mud/ooze, and interpreted this to represent an absence of sedimentation caused by ice shelf coverage.

Similar time breaks have been found in the Glomar Challenger Basin (Bonaccorsi et al., 2000) and in the JOIDES Basin (Brambati et al., 2002). However, in places where it is possible to find, between diamicton and the biogenic siliceous mud/ooze, a sandy mud sediment inferred to represent the glacial/interglacial transition (Brambati, 2000).

Domack et al. (1999) interpreted this sequence according to Walther's law as a succession of facies recording the transition from sub-glacial to open marine environments: a) a massive diamicton, reflecting a subglacial setting; overlain by b) granulated facies composed of loosely compacted sandy, muddy gravel, reflecting the lift-off of the ice shelf from the sea floor as the grounding line retreated; c) laminated glacio-marine mud, indicating a sedimentation seaward of the grounding line; d) silty clay unit, indicating an ice shelf setting distant from any basal debris (null point: the most distal sites from the grounding line and from the open-marine productivity); e) a detritus rich and coarser from eolian input, iceberg and sea-ice rafting near the calving front of the receding Ross Ice Shelf; and f) diatomaceous mud (ooze), indicating open marine setting.

Table 1
Site information for the cores for this study

Core	Latitude	Longitude	Water depth (m)	Core length (cm)
ANTA96-5bis	75°44.84′S	179°45.55′ W	568	636
PT16	74°44.48′S	179°28.465′E	431	195.5
PT17	75°19.38′S	179°09.64′ W	540	307
PT39	75°36.74′S	179°37.79′ W	568	780.5

Table 2
Analyses carried out on the cores in this study

Analyses	ANTA96-5bis	PT39	PT16	PT17
Radiographs	x	x	x	x
Sediment color	x	x	x	x
VMS	x	x	x	x
Shear Strength	x			
Water content	x			
Grain size	x			
Mineralogical comp.	x			
Organic Carbon and Nitrogen	x			
Foraminifera	x			
Radiocarbon dating	x			

Four cores were collected in the Pennell Trough (Fig. 1; Table 1) during cruises of the M/N Italica between 1995 and 2002. Previous studies carried out on one of the studied cores (ANTA96-5bis) recognized three facies having different sedimentological, compositional, geochemical and micropalaeontological characteristics (Salvi et al., 2000). *Unit a,* at the bottom, is interpreted as a glacial marine diamicton, rich in both siliceous (diatoms, sponge spiculae, radiolarians) and calcareous planktic and benthic foraminifera. The overlying *units b*, *c*, *d,* represent a sediment gravity flow facies with thin layers of sand and muddy sand, lacking foraminifera, rare sponge spiculae, and mainly reworked radiolarians and diatoms (Tolotti, 2002). At the top, *unit e,* made up of siliceous mud/ooze, indicates the open marine biogenic sedimentation and marks the beginning of the Holocene.

Presented herein are additional data on these cores, including X-ray radiographs, volume magnetic susceptibility (VMS), bulk and clay mineral composition, foraminifera and further radiometric dating (Table 2). These results help constrain the palaeoenvironmental changes related to ice-sheet coverage and the transition to open marine conditions.

2. Methods

Radiographs were made at the "Wårtsila Italia s.p.a." facility in Trieste, Italy. A total of 50 negatives 40 cm long, X-ray radiographs and the positive photographs were analyzed. Sedimentary structures were examined and integrated by a visual investigation with the fresh sediment surface. The grain-size was interpreted by grey-scale patterns from sediment responses to the X-ray penetration. Sediment colour was evaluated by

comparison with Munsell's Soil Colour Charts on the fresh sediment surface.

The volume magnetic susceptibility (VMS) was acquired on the split core ANTA96-5bis, with 1 cm of sampling interval by a Multi-Sensor Core Logger (Geotek®), a non-destructive automated system, using a Bartington high resolution surface scanning point sensor MS2EI model, with about 0.4 cm of horizontal resolution. A Bartington Loop Sensor MS2C model was used to scan the other whole cores (PT39, PT16 and PT17) at 2 cm sampling interval with 2 cm of nominal spatial resolution.

The shear strength was determined on 42 samples using a penetrometer with a mean interval of about 20 cm, whereas the water content was determined on 270 samples by weighing and drying (3–4 days at 60 °C) the whole sediment slice. Results are expressed as a percentage of dry sediment weight.

A total of 100 samples were treated with distilled water and wet-sieved to separate gravel (>2 mm), sand (2000–63 μm) and mud (<63 μm) fractions (Wentworth, 1922). The sand fraction was analyzed in a Macrogranometer settling tube while the silt and clay fraction was analyzed on a Sedigraph 5100 particle size analyzer. The sand and mud fraction have been calculated to 100% excluding the gravel content.

Mineralogical composition of the bulk sediment and clay-size (<2 μm) fractions were determined for 70 samples (core ANTA96-5bis) through X-ray "powder" diffraction (XRD) using a Philips PW 1800 diffractometer with CuKα radiation with about 5–10 cm sample spacing. For the analyses of bulk mineralogy, the relative peak heights were estimated from the main reflections of the diffraction curve. In addition, the amorphous content (biogenic silica) of the bulk sediment was estimated by measuring the area of diffuse scatter in each X-ray pattern (a methodology similar to Cook et al., 1975). For analyses of clay minerals, the <2 μm fraction was separated by settling in a distilled water column. Samples were mounted as oriented aggregates on glass slides. The diffractograms were recorded in natural conditions (air-drying) and after treatment in ethylene glycol. Semi-quantitative analysis was performed according to Biscaye (1965). Illite chemistry was also calculated from the 5/10 Å intensity ratio (Esquevin, 1969). The ratio decreases with Mg and Fe substituting for octahedral Al, with values higher than 0.4 being typical of muscovite, while those lower than 0.15 are associated with biotite.

The organic carbon and nitrogen content was determined using a Perkin-Elmer 2400 CHNS/O Elemental Analyzer on 100 samples. About 10–20 mg of sediment was used and the carbonate fraction was dissolved using hydrochloric acid in silver capsules (Hedges and Stern, 1984).

Table 3
Uncorrected radiocarbon ages for core ANTA96-5bis

Depth (cm)	$\delta^{13}C$ (‰)	Uncorrected radiocarbon age (yr)
0–2	−30.6	3820 ± 40
84–86	−25.8	24,740 ± 110
90–92	−25.7	21,820 ± 210
190.5–192	−25.4	27,270 ± 410
339–342	−25.0	27,370 ± 400
450–453	−26.1	37,000 ± 1400

For micropalaeontological analyses the whole core was examined in 2 cm thick samples. For the benthic and planktic foraminifera all the specimens per sample are counted. The silica taxa (diatoms, radiolarian and sponge spiculae) are reported as abundant, common or rare.

Radiocarbon ages were determined on decalcified organic carbon using Accelerator Mass Spectrometry (AMS) via the Geochron Laboratories (Massachusetts, U.S.A.). Ages are reported as uncorrected values except for adjustment due to $\delta^{13}C$ fractionation (Table 3).

3. Core lithofacies

We identify three main lithofacies, diamicton, sediment gravity flow deposits and diatomaceous mud/ooze.

From X-ray analysis and VMS peaks correlation (Fig. 2) the cores PT39 and ANTA96-5bis resemble the same sequences of lithofacies. Core PT39 contains diamicton in the interval from 780 (bottom) to 420 cm. Between 420 to 90 cm the sediment consists of homogeneous mud with sand-and gravel-bearing intervals at 400–370 cm and 216–160 cm. The latter interval is characterized by upward grading in the coarse fraction (coarse tail grading).

From 90 cm to the top of the core the sediment is characterized by a homogeneous diatomaceous mud (silica content 10%–30%) and ooze (silica content >30%).

Core ANTA96-5bis contains diamicton from the base at 638 cm to 450 cm. From 450 to 70 cm the facies is mainly structureless mud with two significant coarse layers. The lower one, from 450 to 420 cm, is inversely graded and composed of pebbles (3–4 cm diameter) overlying a bed of coarse sand with a muddy matrix. The second layer, from 190 to 170 cm, is less well organized, though coarsening upward from sand to pebbles was observed. The upper part of the core is made up of diatomaceous mud/ooze with pervasive bioturbation (Salvi et al., 2000). Core PT16 is

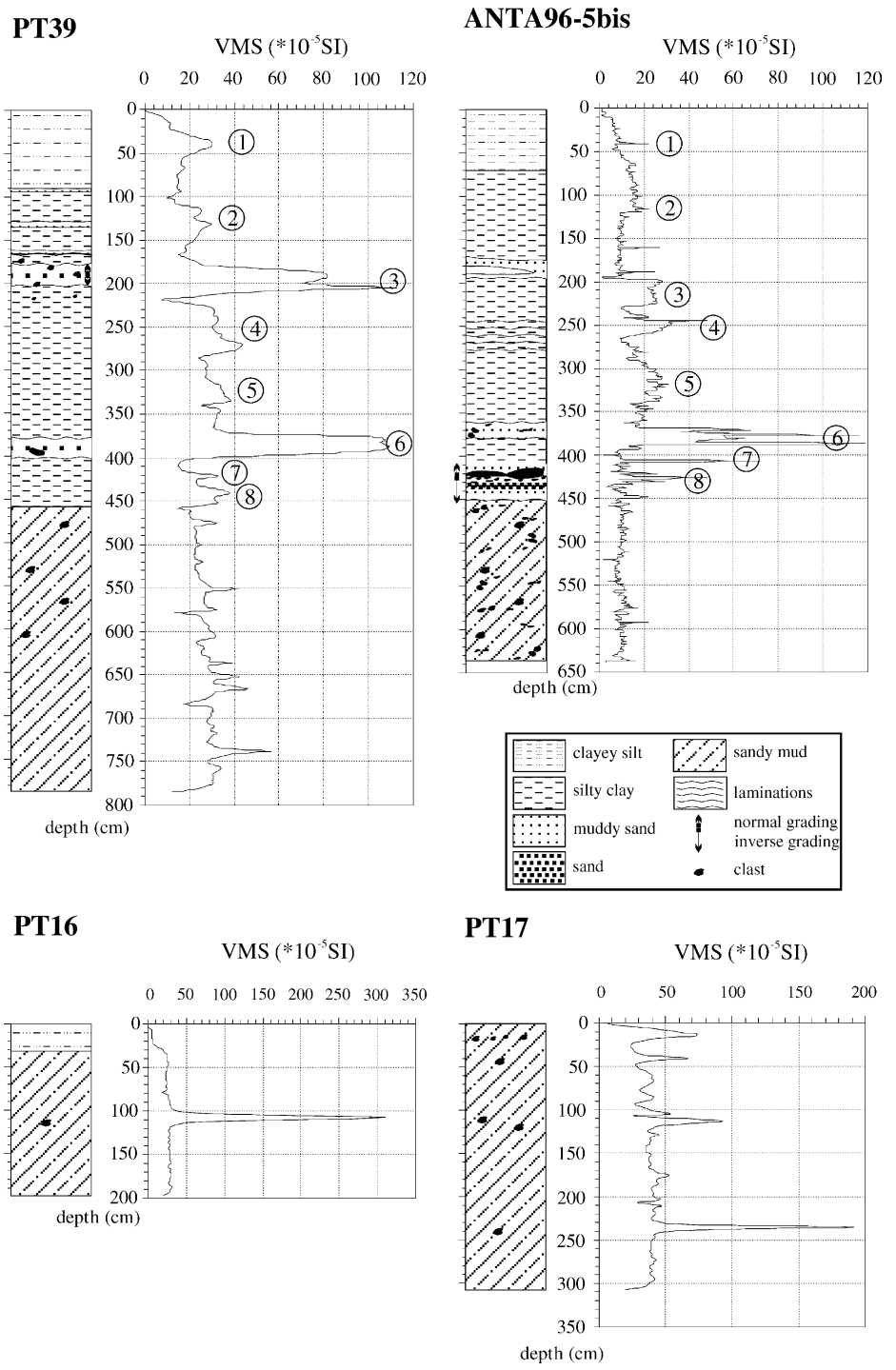

Fig. 2. Lithology and volume magnetic susceptibility (VMS) of the cores. The circled numbers identify corresponding peaks in volume magnetic susceptibility in cores PT39 and ANTA 96-5bis.

characterized by a diamicton from bottom (200 cm) to 30 cm, where it is overlain by diatomaceous mud/ooze. Diamicton is also present in the core PT17 from the bottom (305 cm) to 20 cm, but here the topmost part (0–20 cm) contains normally graded gravelly sand, bearing many unsorted clasts up to 3 cm.

The average values of VMS (Fig. 2) for all the four studied cores range between 20 and 40*10^{-5}SI with

peaks up to $120/130 \times 10^{-5}$ SI in some particular layers of cores PT39 and ANTA96-5bis and peaks up to $200/300 \times 10^{-5}$ SI, in cores PT16 and PT17 due to the presence of big clasts. The VMS peak correlations between cores PT39 and ANTA96-5bis are assumed to link the same horizons.

The results of our analyses maintain the subdivision of ANTA96-5bis into the five *units* established by Salvi et al. (2000). All the other measured parameters, X-rays, organic carbon, C/N ratio, water content, VMS and mineralogical composition support this stratigraphic subdivision, which is described in more detail below.

3.1. Unit a (diamicton)

This *unit* (638–450 cm) is characterized by homogeneity in most parameters. The sediment (diamicton) is dark olive grey (5y 3/2) structureless clay-silty matrix with dispersed gravel (Fig. 3). Sand, silt and clay proportions are uniform down core with mean values of $15.7 \pm 1.04\%$, $41.6 \pm 1.44\%$ and $42.7 \pm 1.63\%$ respectively, with scarce but constant presence of gravel (<3%). In this unit, the water content values (Fig. 4) are uniformly low, ($42.51 \pm 2.11\%$;). The VMS (Fig. 2) is generally low, with a mean of $9.61 \pm 2.27 \times 10^{-5}$ SI. The shear strength (Fig. 4) values are the highest recorded in the core (mean of 1.29 ± 0.25 kg/cm^2) although values are always <2 kg/cm^2.

In the bulk sediment (Fig. 5), the content of biogenic silica is high, indicating an abundance of siliceous detritus.

The values of the ratio quartz/mica, quartz/chlorite and feldspars/mica, are low with some fluctuations in the lower part; feldspars are the most abundant silicate, quartz and mica are present in similar amounts while chlorite is subordinate (Fig. 5).

The clay mineral assemblage (Fig. 6), is composed mainly of illite (50%–60%) with chlorite up to 20% and smectite <20%. Smectite contents are the lowest of the whole core, while those of chlorite are the highest. High values of 5/10 Å ratio of illite indicate this mineral can be classified as muscovite.

Agglutinated foraminifera (*Trochammina multiloculata*) is rare. The presence of well-preserved marine taxa like diatoms, sponge spicules, radiolarian and foraminifera both benthic (*Astrononion antarticus* and *A. echolsi*, *Cibicides refulgens*, *Ehrenbergina glabra*, *Globocassidulina biora, G. crassa* and *G. subglobosa*, *Trifarina angulosa*, etc.) and planktic (*Neogloboquadrina pachyderma*), suggests that the CCD was at lower depth or a paucity of organic matter led to a minimal pore water acidity (see Supplementary data).

Total organic carbon shows low and constant values around 0.4% (mean value of $0.44 \pm 0.02\%$), comparable with other diamictitic sediments in the continental shelf of the Antarctic (Domack et al., 1999; Domack and McClennen, 1996; Brambati et al., 1997; Licht et al., 1999). The nitrogen values are quite uniform (mean $= 0.04 \pm 0.004\%$) and C/N ratios are high, with a mean of 11.78 (Fig. 7).

Radiocarbon dating (Fig. 4; Table 2), indicates an age for this unit of >37,000 years BP (Salvi et al., 2000).

3.2. Unit b (muddy sand with gravel)

A sharp contact marks the base of this *unit* (450–380 cm) characterized by a dark grey (5y 4/1) inversely graded interval (450–420 cm), as indicated by both radiographs and grain-size data. This interval is composed of coarse sand with a muddy matrix overlain by pebbles of 3–4 cm diameter (Fig. 3). The pebble content decreases from 420 to 396 cm, the bulk of the interval being characterized by a grey (5y 5/1) silty clay, while from 396 to ~ 380 cm a dark grey layer with abundant pebbles and sand is present.

The water content has two minimum values, 18.0% at 422 cm and of 34.4% at 380 cm with a mean of $39.8 \pm 16.1\%$. The shear strength at 391.5 cm is 0.56 kg/cm^2 (Fig. 4).

Between 450 and 380 cm depth the VMS values (Fig. 2) are still low ($12.00 \pm 10.25 * 10^{-5}$SI) but less uniform compared to *unit a.* There is a general increase in the sand and gravel fractions with a mean value of $35.6 \pm 22.6\%$ and $4.5 \pm 6.8\%$, respectively. The mud component has a mean value of $60.0 \pm 25.5\%$ (Fig. 5).

The biogenic silica content reflects the grain size, as the values decrease abruptly around 400 cm depth, corresponding to an increased sand content. Also the ratios quartz/mica, feldspars/mica and quartz/chlorite reflect the presence of coarse-grained sediment, as high values are observed around 400 cm (Fig. 5). This indicates an increase in quartz and decrease in other minerals. In the clay fraction, smectite comprises 25%–50%, illite 35%–55% and chlorite 13%–20% (Fig. 6). Smectite increases within *unit b* with respect to *unit a*, and a strong peak (up to 50%) is present between 400 and 450 cm.

In *unit b* a decrease in carbon content (mean value of $0.16 \pm 0.08\%$) is observed, while the nitrogen values are quite uniform (mean $= 0.02 \pm 0.01\%$). C/N ratio shows high values with a mean of 10.4 ± 4.6 (Fig. 7).

From 450 to 380 cm foraminifera are absent and the siliceous taxa are rare. (Table 3).

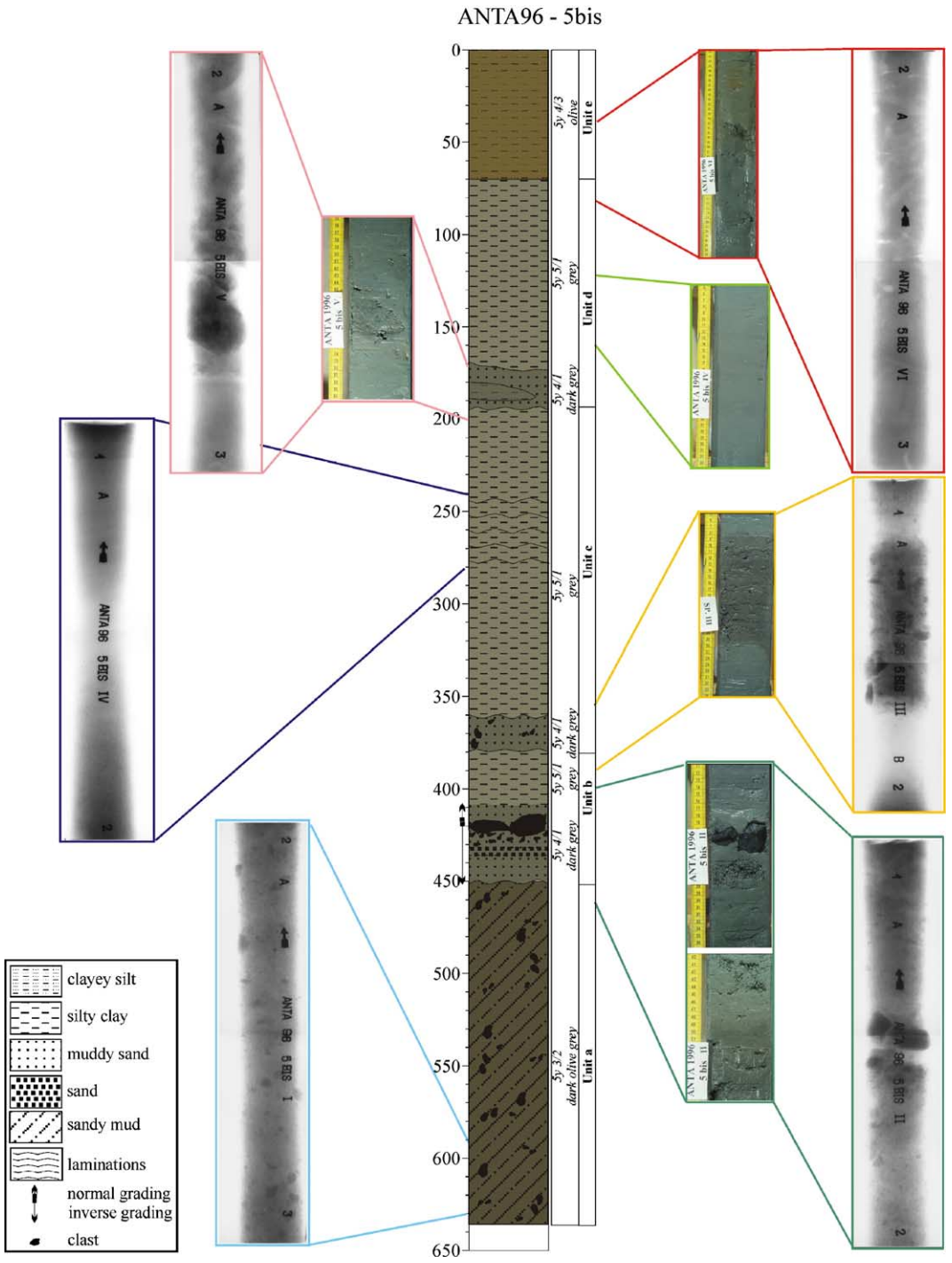

Fig. 3. Lithology of the core ANTA96-5bis, with X-rays and photographs of the most representative facies. The *unit a* (638–450 cm) is characterized by a sandy mud with sparse pebbles (IRD) glacial-marine diamicton. The *units b*, *c*, *d* (450–70 cm), are characterized by different gravity flow events, with an erosive boundary at the base of each. This interval is characterised by an homogeneous silty clay with occasional laminations. The upper part of the core, *unit e* (70–0 cm), is a bioturbated diatom mud/ooze.

The sharp undulating contact between *units a and b* and the general characteristics of *unit b* suggest this is a sediment gravity flow. Moreover the inversely graded interval observed from 450 to 420 cm can also be interpreted, following Shanmugam (2000) as a "sandy debris flow". The author notes that only debris flows can de-

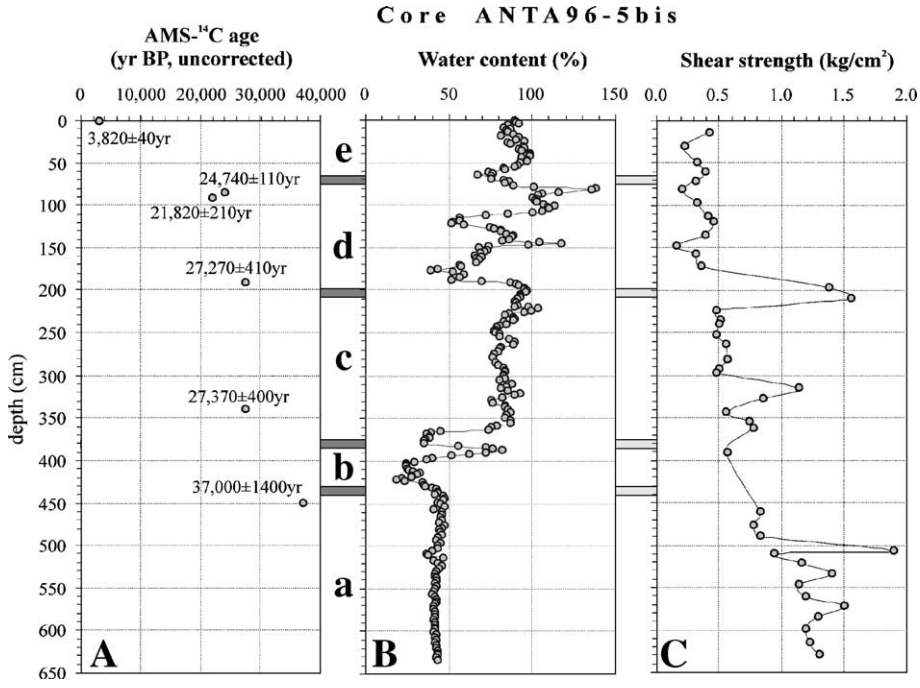

Fig. 4. Radiocarbon age (AMS-^{14}C age uncorrected), water content, expressed as a percent of dry sediment weight and shear strength (kg/cm^2) of core ANTA96-5bis.

velop inverse grading, whereas turbidity current deposits show only normal grading. The author also notes that a minimum of 25% of sand and gravel is typically needed to generate a sandy debris flow - in the basal part of *unit b* the sand and gravel content is 50-60%.

3.3. Unit c (silty clay)

This *unit* (380–190 cm) is nearly structureless with sparse small mud chips in a grey (5y 5/1) muddy matrix. Occasionally faint planar to oblique lamination is present (Fig. 3). From 380 to 190 cm the water content values are uniform, with a mean of 80.3 ± 15.8%. This unit is characterized by a decrease in shear strength with a mean value of 0.73 ± 035 kg/cm^2 and two peaks at 314.5 cm of 1.13 kg/cm^2 and between 197.5–209.5 cm of 1.46 ± 0.12 kg/cm^2 (Fig. 4).

Three sub-intervals based on VMS are observed: from 380–265 cm, 265–230 cm and 230–197 cm with mean values of 24.4 ± 14.9, 21.63 ± 8.94 and 23.94 ± 2.8 × 10^{-5} SI, respectively. From 388 to 368 cm VMS is highest with a mean of 59.00 ± 23.66 × 10^{-5} SI, and peaks of 119 and 116 × 10^{-5} SI, in correspondence with muddy sand interval (Fig. 2).

Unit c is characterized by the lowest percentage of sand (mean: 2.7 ± 6.5%) of the whole core, with an absence of gravel. The mud fraction is mostly clay, (mean of 63.0 ± 8.4%), whereas the silt has a mean of 34.4 ± 5.5% (Fig. 5). In the bulk sediment, biogenic silica is high and constant, while the values of the ratio quartz/mica, quartz/chlorite and feldspars/mica are low (Fig. 5). The clay mineral assemblage is rather homogeneous and similar to *unit b* (Fig. 6). *Unit c* is characterized by a mean value of carbon content of 0.3 ± 0.05%. Minimum values of nitrogen were observed with a mean of 0.04 ± 0.01% while C/N ratio presents high values with a mean of 9.1 ± 3.7 (Fig. 7). The biogenic content reaches 10% and is made up exclusively of silica, especially of radiolaria, sponge spicules and diatoms, while foraminifera are present 380–330 cm (see Supplementary data). Uncorrected AMS ages from *unit c* are 27,370 ± 400 years BP (339–342 cm depth near the bottom of the unit) and 27,270 ± 410 years BP (190.5–192 cm depth at the top of the unit).(Fig. 4; Table 3). This, together with the sedimentological and geochemical results, support the hypothesis of a single turbidite event.

3.4. Unit d (mud)

A sharp boundary delimits the lower uniform muddy *unit c* from this *unit* (190–70 cm), characterized by big mud chip, chaotic increase of pebbles and sand fractions. Upwards the pebble content decreases while a

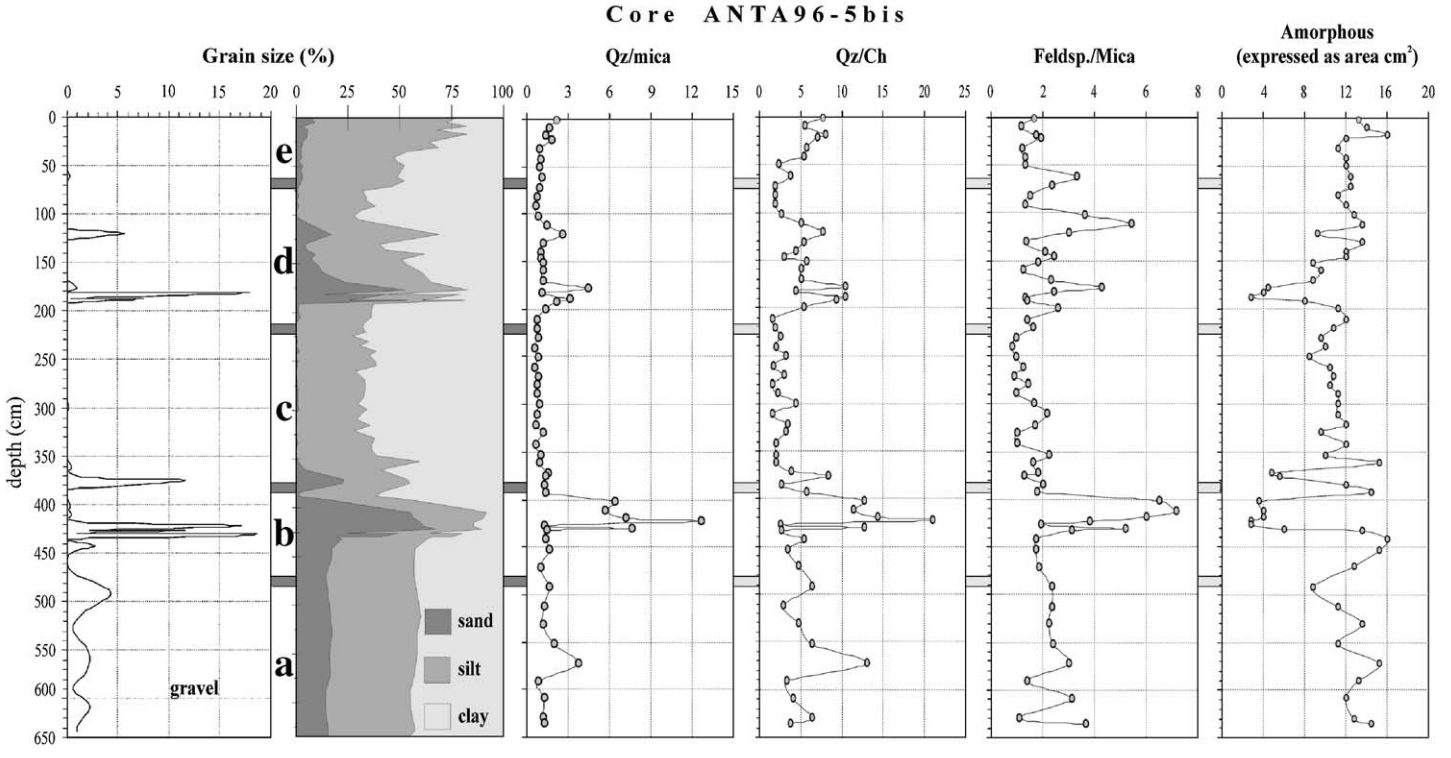

Fig. 5. Grain size distribution (%), quartz/mica, quartz/chlorite and feldspar/mica ratio and amorphous biogenic silica expressed as area (cm2) of core ANTA96-5bis.

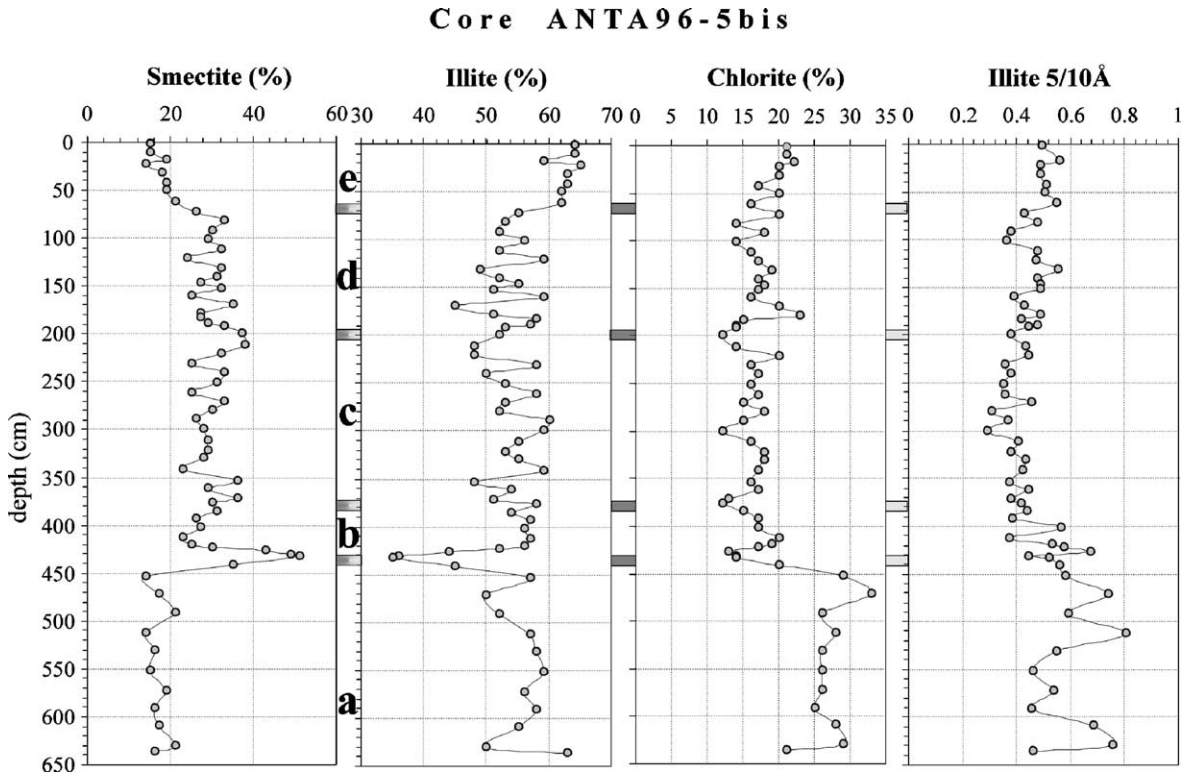

Fig. 6. Clay mineral composition of smectite, illite and chlorite (%) of core ANTA96-5bis.

few millimeter-size grains still occur. This interval shows no evidence of bioturbation nor primary sedimentation structures (Fig. 3).

The water content values are irregular with a mean of $80.7 \pm 22.0\%$ and three minimum at 177 cm (39.0%), at 122 cm (51.5%) and at 65 cm (66.4%).

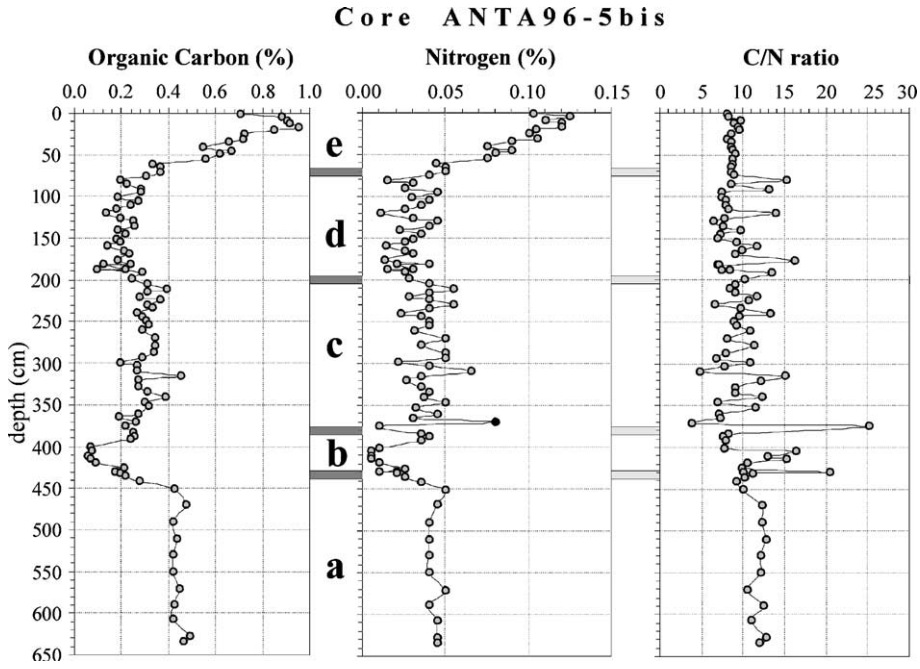

Fig. 7. Total organic carbon (TOC), nitrogen (N) and C/N ratio distributions in core ANTA96-5bis.

The shear strength is low with a mean value of 0.32 ± 0.09 kg/cm^2 (Fig. 4). VMS is quite uniform with a mean of $9.67 \pm 3.37 \times 10^{-5}$ SI (Fig. 2). In this unit an increase of the coarse fraction is evident with $2.32 \pm 5.07\%$ of gravel and $20.54 \pm 18.07\%$ of sand. Clay and silt proportions are quite variable with a mean of $37.20 \pm 9.78\%$ and $39.93 \pm 17.24\%$, respectively (Fig. 5). In the bulk sediment, chlorite and mica are present in lower amounts than in *unit c* whereas quartz and feldspar increase. The content of biogenic silica fluctuates and low values are present between 150 and 200 cm (Fig. 5). The mineralogical composition of the clay fraction is similar to that of *units c* and *b* (Fig. 6).

In this unit there is a decrease of TOC, with a mean percentage of $0.20 \pm 0.06\%$ while minimum values of nitrogen are observed (mean $= 0.027 \pm 0.01\%$). In this unit the values of C/N ratio decrease up core with a mean of 9.5 ± 3.16 (Fig. 7).

Siliceous taxa are quite variable with percentages between 40% toward the upper part of the unit, and 5% around 150–190 cm, while foraminifera are rare (see Supplementary data).

Uncorrected AMS datings reveal an age of 24,740 ± 110 years BP at the top of *unit d* overlying younger sediments aged $21{,}820 \pm 210$ years BP (Fig. 4; Table 3). This suggests the presence of reworked sediment. According to the sedimentological analysis *unit d* represents another sediment gravity flow, probably a turbiditic event.

3.5. Unit e (biosiliceous mud/ooze)

The upper part of the core (70–0 cm) is characterized by olive (5y 4/3) muddy sediment with abundant bioturbation (Fig. 3). Water content is uniform with a mean value of $90.0 \pm 5.18\%$. The shear strength is low with a mean of 0.33 ± 0.08 kg/cm^2 (Fig. 4). The VMS, from 120 to 0 cm, exhibits a decreasing trend towards the top with a mean of $11.2 \pm 4.92 \times 10^{-5}$ SI (Fig. 2). This unit is characterized by the highest mean percentage of silt fraction ($56.3 \pm 16.89\%$) in the core and by a rather high percentage of clay ($40.9 \pm 18.03\%$). The sand fraction is very low ($2.7 \pm 2.02\%$) while gravel is completely absent (Fig. 5).

In the bulk sediment, the content of biogenic silica is high and rather homogeneous. The values of the ratios quartz/mica, quartz/chlorite and feldspars/mica in the upper part are high but decrease downcore; their trend mirrors that of silt content (Fig. 5). In the clay fraction smectite is lower than *unit d* (<20%) and increases downcore, illite shows the highest amount of the whole core (up to 65%), whereas chlorite is between 10%–15% (Fig. 6).

Unit e shows a dramatic increase in TOC from 0.3% at the base to >0.9% in the top 20 cm (Fig. 7), and there is a similar increase of nitrogen from 0.04% to 0.12%, indicating the beginning of open marine conditions (Domack et al., 1999).

This unit is characterised by an abundance of foraminifera. The benthic fraction consists of mainly agglutinated foraminifera (*Cribrostomoides wiesneri*, *Lagenammina difflugiformis*, *Miliammina earlandi*, *M. lata* and *M. oblique*, *Pseudobolivina antartica*, *Reophax scorpiurus*, etc.), but calcareous foraminifers are also present (*Astrononion echolsi*); the planktonic forams are characterised always by *Neogloboquadrina pachyderma* (see Supplementary data). Biogenic silica is very high and mainly made up by sponge spicules, with subordinate diatoms and radiolarians.

These observations from *unit e* reflect a warmer climate condition and retreat of permanent ice, resulting in a higher biological productivity. The top of the core is dated 3820 ± 40 years BP, which is close to agreement with core top ages reported by others (Licht et al., 1996; Domack et al., 1999). Considering the small thickness of *unit e* (70 cm) and the much older radiocarbon ages for *unit d* ($21{,}820 \pm 210$/$24{,}740 \pm 110$ yr BP) we presume a very low sedimentation rate, or even a hiatus, in line with the interpretation of Domack et al. (1999) for such a boundary as a null point, being most distal from both the grounding line and from the open-marine productivity, and hence sediment starved. A hiatus at the base of *unit e* would be consistent with time breaks in other cores from Ross Sea (Licht et al., 1996), where no deposition occurred between approximately 20,000 and 7000 years BP.

4. Discussion

These cores have provided a record of the glacial evolution of the basin over the last 37,000 years. The identification in the core ANTA96-5bis of a glacial marine diamicton indicates that grounded ice was not present at that time in the central and deepest part of the Pennell Trough, confirming the view of Howat and Domack (2003) from seismo-stratigraphic evidence. Diamicton from the Ross Sea continental shelf which exhibits shear strength values exceeding 2.5 kg/cm^2 (Anderson et al., 1980) is interpreted as being “basal till” (Anderson and Molnia, 1989). In this case the presence of well-preserved planktic foraminifera and the constant TOC values around 0.4% (Licht et al., 1999) and shear strength values consistently below 2

kg/cm^2 suggest that the ice was not grounded on the floor of the basin. All of these features permit us to interpret the lower unit of the core ANTA96-5bis as a "glacial marine diamicton" (Licht et al., 1996, 1999).

This represents the first sedimentological evidence of the hypothesis of Shipp et al. (1999) and Howat and Domack (2003), that the depocenter of the Pennell Trough was partially free of grounded ice during the last glacial period. We infer a 3.5-m-thick sediment gravity flow deposited on the glacial marine diamicton proximal to the grounding line (Fig. 8), as exemplified in cores ANTA96-5bis and PT39 (Figs. 8). This was followed by debris flows and turbidity currents triggered by ice sheet movement during or immediately following the LGM. Similar gravity flow deposits are recognized in other basins in the Ross Sea (Kurtz and Anderson, 1979; Anderson et al., 1984; Bonaccorsi et al., 2000). The presence of morphological escarpment with a gradient of about 150 m in 10 km, about 35 km west of the cores, interpreted as a subglacial delta (Anderson and Bartek, 1992) or as lateral moraine (Domack et al., 1999), and the occurrence of back-stepping moraine ridges (Shipp et al., 1999; Howat and Domack, 2003) might represent a further source of sediment for these gravity flows.

The ages determined from these deposits date the sediment source rather than the time of redeposition and are in fact somewhat older than the LGM, but this is still consistent with their redeposition at that time (around 18,000 years BP, Pisias et al., 1984).

This hypothesis is supported by the ages of the core ANTA96-5bis. Coeval ages of about 27,000 years BP date a sediment gravity flow event in *unit c*, overlying a sandy debris flow (*unit b*), followed by thick layer of mud and a second sediment gravity flow (*unit d*) with a reversed ages (24,740 years BP over 21, 820 years BP). Moreover the paucity of foraminifera and silica taxa in the interval and the presence of a cold water diatom assemblage in *unit d* with increase of *F. obliquecostata* (Tolotti, 2002) suggest environmental conditions of permanent ice cover to the top of *unit d* (Fig. 8B).

Around 8000 years BP, following a time break as argued in the previous section, diatom mud/ooze began accumulating through the retreat of the ice shelf from the shallow banks of the middle shelf, as recorded by Hilfinger et al. (1995) and Domack et al. (1999). This mud/ooze is characterized by diatoms such as *F. curta* and *F. obliquecostata*, which indicate winter sea ice and summer open marine conditions (Tolotti, 2002). The lack of calcareous foraminifera suggests that the CCD rose to shallower water depths (Kellogg et al., 1979; Osterman and Kellogg (1979). This in turn increased the primary productivity with a resulting higher accumulation of organic matter, and a rise of CO_2 content in the water. It is noteworthy that at the present time the winter sea ice completely covers the Ross Sea south of 70° S, and that during the summer when the melting of sea ice starts, the western Ross Sea is a polynya, being separated from the Southern Ocean by a belt of sea ice. The increase of the organic carbon in *unit e*, and hence productivity, reflects a progressive transition to these relatively warm climatic conditions and regular periods of open water.

The mineral composition of the clay fraction of core ANTA96-5bis is composed of abundant illite and subordinate smectite and chlorite, an assemblage that is typical of marine sediments around Antarctica (Chamley, 1989; Ehrmann et al., 1992). Clay mineral distribution and VMS appear to reflect the main lithostratigraphic units, as their relative percentages are distinctly different in the lower, intermediate and upper parts of the core (Fig. 6). Different clay mineral assemblages cannot be attributed to variations in the intensity of chemical or physical weathering processes on land, which has been largely ice-covered for the last several million years at least. Therefore the clay mineral assemblages more likely highlight the different provenance of sediment deposited at different times. For the identification of the parent rocks, a detailed description of the present distribution of clay minerals in the basin would be required, but does not exist. However, it is possible to hypothesize the different provenance of clays on the base of the composition of the surrounding lithologies and the characteristics of the current, as reported in some papers (Ehrmann et al., 1992; Lucchi et al., 2002; Marinoni et al., 2000). Smectite can be present in high contents in Quaternary sediments from Ross Sea as a product of alteration of basic volcanic lithologies, (Ehrmann et al., 1992; Ehrmann, 1998) in

Fig. 8. Proposed palaeoenvironmental evolution model of the Pennell Trough. (A) Glacial period (late Wisconsinan): grounded ice was present on the highs surrounding the Pennell Trough but not in the depocenter where glacial marine diamicton was being deposited from 37,000 ± 1,400 yr BP on. (B) During the LGM advance grounded ice mobilized sub-glacial diamicton, triggering turbidity currents and debris flows. (C) After the LGM and during the transition to the present interglacial period the basin was starved of sediment through retreat of the grounding line and the ice shelf margin. This prevented terrigenous sediment from being carried offshore, and multiyear sea-ice cover lowered productivity and hence reduced biogenic supply. However there may have been occasional periods of open marine conditions. (D) The Holocene climatic amelioration with open marine conditions in summer increased productivity that led to the deposition of the diatomaceous mud/ooze.

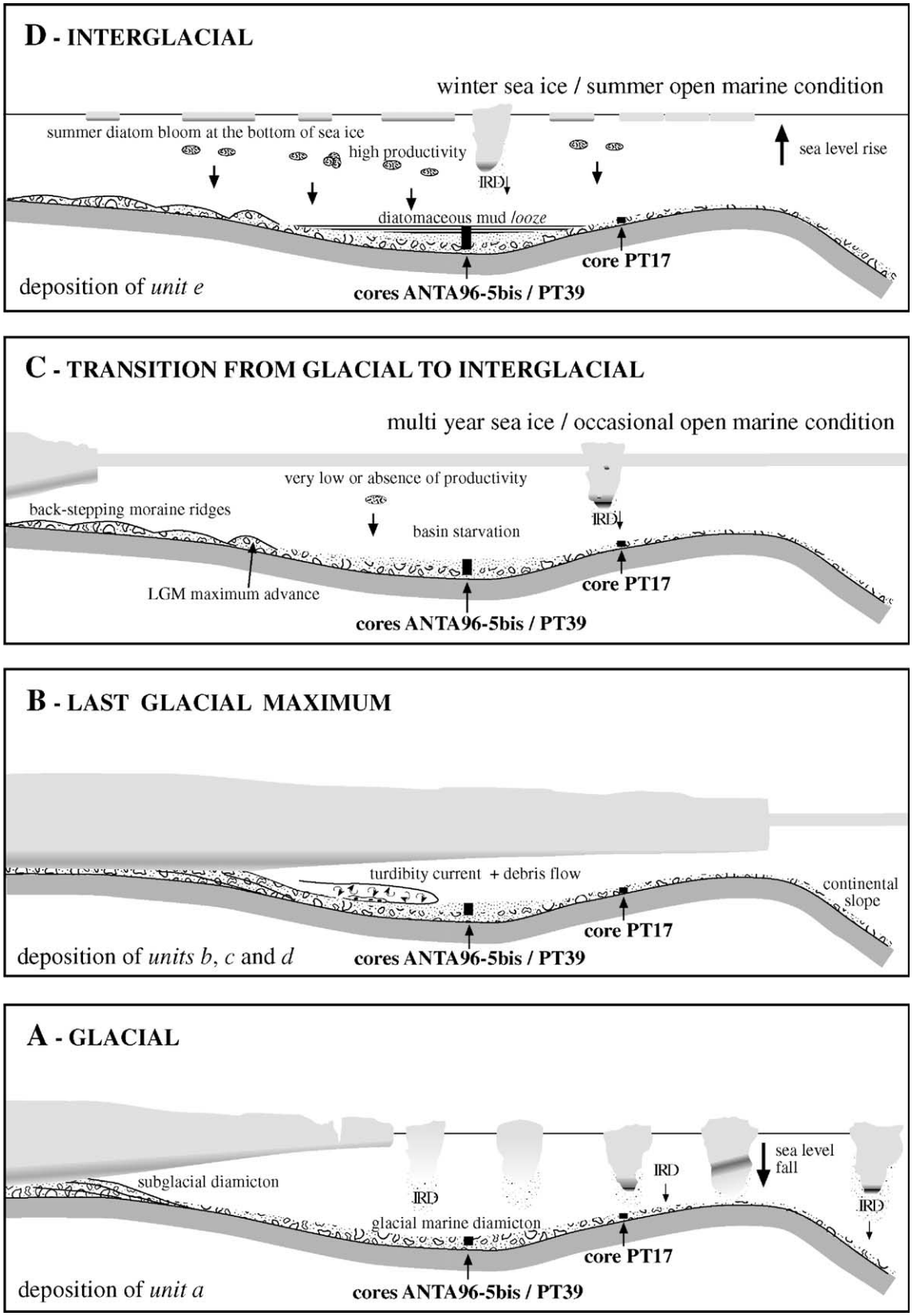
D - INTERGLACIAL
winter sea ice / summer open marine condition
summer diatom bloom at the bottom of sea ice
high productivity
IRD
sea level rise
diatomaceous mud looze
core PT17
deposition of unit e
cores ANTA96-5bis / PT39
C - TRANSITION FROM GLACIAL TO INTERGLACIAL
multi year sea ice / occasional open marine condition
very low or absence of productivity
back-stepping moraine ridges
basin starvation
IRD
LGM maximum advance
core PT17
cores ANTA96-5bis / PT39
B - LAST GLACIAL MAXIMUM
turdibity current + debris flow
continental slope
core PT17
deposition of units b, c and d
cores ANTA96-5bis / PT39
A - GLACIAL
subglacial diamicton
IRD
IRD
sea level fall
IRD
glacial marine diamicton
core PT17
deposition of unit a
cores ANTA96-5bis / PT39

particular from the McMurdo Volcanic Group, which has volcanic centres along the Victoria Land coast extending from Mt Morning to Cape Adare (Kyle, 1990). Illite and chlorite might derive from the lithologies outcropping on the East Antarctic Craton. Chlorite generally occurs in low-grade metamorphic and basic lithologies and is not resistant against chemical weathering and transport, while illite tends to derive from more acid lithologies and it is more resistant (Biscaye, 1965; Chamley, 1989; Ehrmann, 1998 and references therein).

The high illite and chlorite contents in the core, but in particular in *units a* and *e,* likely indicate provenance from the East Antarctic interior. This provenance is supported by the increase of illite 5/10 Å in *unit a*. Higher values of the ratio indicate an increase of muscovite with respect to biotite type and, therefore, a provenance from more acidic parent rocks. In the sediment gravity flow intervals (*unit b*, *c* and *d*) the high smectite content probably indicates an increase in the contribution from volcanic centres along the Victoria Land coast.

5. Conclusions

The transition from Late Pleistocene glacial period to the Holocene open marine conditions have been identified in cores from the floor of the Pennell Trough in the northwest corner of the Ross Sea through the identification of three main facies:

1) Glacial marine diamicton (*unit a* – >37,000 yr BP) – This facies was recognized on the basis of homogeneity in all the examined parameters (sedimentological, geochemical, mineralogical, physical properties and so on), low shear strength (<2 kg/cm^2) and water content, and from the presence of autochthonous calcareous foraminifera. These features suggest that during the last glacial period (Late Wisconsinan) the ice was not grounded to the sea floor of the depocenter of the basin but it was anchored on the surrounding highs. These observation are in agreement with the interpretation of Shipp et al. (1999) and Howat and Domack (2003) but in contrast with those of Licht et al. (1996, 1999), that located the grounded ice up to 74° S, while the core is at about 75°45′S.
2) Sediment gravity flow (*units b, c, d* – ~27,500/22,000 yr BP) – This facies is interpreted to have come from glacial advances during the last glacial maximum that mobilized glacial marine/subglacial deposits along the flanks of the basin. Acoustic facies studies (Shipp et al., 1999; Howat and Domack, 2003) support this hypothesis. Sediment gravity flows are found in the cores proximal to the grounding line, but are absent in cores located in the distal area and on the eastern flank of the basin. The increase of smectite content, a signature for a McMurdo Volcanic Group source, suggests that in the Pennell Trough the glacial provenance during the LGM had consistent contributions from volcanic centres along the Victoria Land coast.
3) Siliceous mud/ooze (*unit e* – 3000 yr BP) – The transition from glacial to interglacial times is characterized by an extremely low sedimentation rate or depositional hiatus. We suggest that basin starvation occurred by a) retreat of the ice shelf grounding line south after LGM, reducing terrigenous supply and b) very low biogenic productivity due to floating shelf ice or multi year sea ice with only occasional open marine conditions. The Holocene climatic amelioration and the following summer open marine conditions increased the productivity that led to the deposition of the diatomaceous mud/ooze.

Acknowledgments

This research was carried out within the framework of the "Glaciology and Paleoclimatic" project supported by the Italian *Programma Nazionale di Ricerche in Antartide* (PNRA).

We thank Renata Giulia Lucchi, Mark Hemer, Eugene Domack and Peter Barrett for their comments and useful suggestions, which helped us to significantly improve the manuscript, and Cristiano Landucci for providing assistance in preparing pictures.

Appendix A. Supplementary data

Supplementary data associated with this article can be found, in the online version, at doi:10.1016/j.palaeo.2005.07.034.

References

Anderson, J.B., Bartek, L.R., 1992. Cenozoic glacial history of the Ross Sea revealed by intermediate resolution seismic reflection data combined with drill site information. In: The Antarctic Palaeoenvironment: A Perspective on Global Change, Antarctic Research Series, vol. 56. American Geophysical Union, Washington, D.C., pp. 231–263.

Anderson, J.B., Molnia, B.F., 1989. Glacial marine-sedimentation. 28th Int. Geological Congress, 1989, Washington, Short Course in Geology, vol. 9. American Geophysical Union, Washington, D.C., pp. 1–127.

Anderson, J.B., Kurtz, D.D., Domack, E.W., Balshaw, K.M., 1980. Glacial and glacial marine sediment of the Antarctic continental shelf. Journal of Geology 88, 399–414.

Anderson, J.B., Brake, C.F., Myers, N.C., 1984. Sedimentation on the Ross Sea continental shelf, Antarctica. Marine Geology 57, 295–333.

Anderson, J.B, Shipp, S., Bartek, L.R., Reid, D.E., 1992. Evidence for a grounded ice sheet on the Ross Sea continental shelf during the Late Pleistocene and preliminary paleodrainage reconstruction. In: Elliot, D.H. (Ed.), Contributions to Antarctic Research III, Antarctic Research Series, vol. 57. American Geophysical Union, Washington, D.C., pp. 39–62.

Biscaye, P.E., 1965. Mineralogy and sedimentation of recent deep sea clay in the Atlantic Ocean and adjacent seas and oceans. Geological Society of America Bulletin 76, 803–832.

Brambati, A., 2000. Palaeoclimatic and palaeoenvironmental records in sediments from the Southern Ocean (Strait of Magellan and Ross Sea). In: Brambati, A. (Ed.), Proceedings of the Workshop "Paleoclimatic Reconstructions from Marine Sediments of the Ross Sea (Antarctica) and Southern Ocean, Terra Antarctica Reports, vol. 4, pp. 1–41.

Brambati, A., Fanzutti, G.P., Finocchiaro, F., Melis, R., 1997. Paleoenvironmental record in core ANTA91-30 (Drygalski Basin, Ross Sea, Antarctica). In: Barker, P.F., Cooper, A.K. (Eds.), Geology and Seismic Stratigraphy of the Antarctic Margin, Part 2, Antarctic Research Series, vol. 71. American Geophysical Union, Washington, D.C., pp. 137–151.

Brambati, A., Corradi, N., Finocchiaro, F., Giglio, F., 2002. The position of the Last Glacial Maximum grounding line in the JOIDES Basin: an interpretation based on sedimentological and geotechnical data. In: Gamble, J.A., Skinner, D.N.B., Henrys, S. (Eds.), Antarctica at the Close of a Millennium. Proceedings of the 8th International Symposium on Antarctic Earth Sciences, Wellington, 1999, The Royal Society of New Zealand Bulletin, vol. 35, pp. 365–372.

Bonaccorsi, R., Brambati, A., Busetti, M., Fanzutti, G.P., 2000. Relationship among X-ray Lithofacies, Magnetic Susceptibility, P-wave Velocity and Bulk Density in Core ANTA95-89C (Ross Sea, Antarctica): first results. In: Brambati, A. (Ed.), Proceedings of the Workshop "Paleoclimatic Reconstructions from Marine Sediments of the Ross Sea (Antarctica) and Southern Ocean", Terra Antarctica Reports, vol. 4, pp. 241–258.

Chamley, H., 1989. Clay Sedimentology. Springer, pp. 1–623.

Cook, H.E., Johnson, P.D., Matti, J.C., Zemmels, I., 1975. Methods of sample preparation and X-ray diffraction data analysis, X-ray mineralogy laboratory, Deep Sea Drilling Project, University of California, Riverside. In: Hayes, D.E., Fraches, L.A. (Eds.), Initial Reports of the Deep Sea Drilling Project, vol. 28. US Government Printing Office, Washington, D.C., pp. 999–1007.

Davey, F.J., 1995. Bathymetry of the Ross Sea. ANTOSTRAT Project, seismic stratigraphic atlas of the Ross Sea, Antarctica. In: Cooper, A.K., Barker, P.F., Brancolini, G. (Eds.), Geology and Seismic Stratigraphy of the Antarctic Margin, Antarctic Research Series, vol. 68. AGU, Washington, D.C., pp. 1–68.

Davey, F.J., 2004. Ross Sea Bathymetry, 1:2,000,000, version 1.0. Institute of Geological and Nuclear Sciences Geophysical Map16. Institute of Geological and Nuclear Sciences Limited, Lower Hutt, New Zealand.

Domack, E.W., McClennen, C., 1996. Accumulation of glacial marine sediments in fjords of the Antarctic Peninsula and their use as Late Holocene palaeoenvironmental indicators. In: Ross, R.M., Hofmann, E., Quetin-Langdon, B. (Eds.), Foundations for ecological research west of the Antarctic Peninsula, Antarctic Research Series, vol. 70. American Geophysical Union, Washington, D.C., pp. 135–154.

Domack, E.W., Jacobson, E.A., Shipp, S., Anderson, J.B., 1999. Late Pleistocene–Holocene retreat of the West Antarctic ice sheet system in the Ross Sea: Part II. Sedimentological and stratigraphic signature. Geological Society of America Bulletin 111 (10), 1517–1536.

Ehrmann, W., 1998. Lower Miocene and Quaternary clay mineral assemblages from CRP-1. Terra Antarctica 5 (3), 613–619.

Ehrmann, W.U., Melles, M., Kuhn, G., Grobe, H., 1992. Significance of clay mineral assemblages in the Antarctic Ocean. Marine Geology 107, 249–273.

Esquevin, J., 1969. Influence de la composition chimique des illites sur la cristallinité. Bulletin du Centre de Recherches de Pau S.N.P.A. 3, 147–154.

Finocchiaro, F., Melis, R., Tosato, M., 2000. Late Quaternary environmental events in two cores from southern JOIDES Basin (Ross Sea, Antarctica). In: Brambati, A. (Ed.), Proceedings of the Workshop "Paleoclimatic Reconstructions from Marine Sediments of the Ross Sea (Antarctica) and Southern Ocean", Terra Antarctica Reports, vol. 4, pp. 125–130.

Giglio, F., Frignani, M., Langone, L., Ravaioli, M., 2000. Palaeoenviromental inferences from Ross Sea gravity cores. In: Brambati, A. (Ed.), Proceedings of the Workshop "Paleoclimatic Reconstructions from Marine Sediments of the Ross Sea (Antarctica) and Southern Ocean", Terra Antarctica Reports, vol. 4, pp. 141–148.

Hedges, J., Stern, J., 1984. Carbon and nitrogen determinations of carbonate-containing solids. Limnology and Oceanography 29, 657–663.

Hilfinger, M., Franceschini, J., Domack, E.W., 1995. Chronology of glacial marine lithofacies related to the recession of the west antarctic ice sheet in the Ross Sea. Antarctic Journal Review 30, 82–84.

Howat, I.M., Domack, E.W., 2003. Reconstructions of western Ross Sea paleo-ice-stream grounding zones from high resolution acoustic stratigraphy. Boreas 32, 56–75.

Hughes, T.J., 1977. West Antarctic ice streams. Reviews of Geophysics 15, 1–46.

Kellogg, T.B., Truesdale, R.S., Osterman, L.E., 1979. Late Quaternary extent of the West Antarctic ice sheet: new evidence from Ross Sea cores. Geology 7, 249–253.

Kyle, P.R., 1990. McMurdo volcanic group – western Ross embayment: introduction. In: LeMasurier, W.E., Thomson, J.W. (Eds.), Volcanoes of the Antarctic Plate and Southern Oceans, Antarctic Research Series, vol. 48. American Geophysical Union, Washington, D.C., pp. 19–25.

Kurtz, D.D., Anderson, G.B., 1979. Recognition and sedimentological description of recent debris flow deposit from the Ross and Weddell Seas, Antarctica. Journal of Sedimentary Petrology 49, 1159–1169.

Licht, K.J, Jennings, A.E., Andrews, J.T., Williams, K.M., 1996. Chronology of late Wisconsin ice retreat from the western Ross Sea, Antarctica. Geology 24, 223–226.

Licht, K.J., Dunbar, N.W., Andrews, J.T., Jennings, A.E., 1999. Distinguishing subglacial till and glacial marine diamictons in the western Ross Sea, Antarctica: implications for a last glacial maximum grounding line. Geological Society of America Bulletin 111, 91–103.

Lucchi, R.G., Rebesco, M., Camerlenghi, A., Busetti, M., Tomadin, L., Villa, G., Persico, D., Morigi, C., Bonci, M.C., Giorgetti, G.,

2002. Mid-Late Pleistocene glacimarine sedimentary processes of a high-latitude, deep-sea sediment drift (Antarctic Peninsula Pacific Margin). Marine Geology 189, 343–370.

Marinoni, L., Quaia, T., Setti, M., Lopez-Galindo, A., Brambati, A., 2000. Mineralogy and crystal-chemistry of the clay fraction in core ANTA91-8 (Ross Sea, Antarctica): palaeoclimatic and palaeoenvironmental implications. Terra Antarctica Reports, vol. 4, pp. 211–216.

Osterman, L.E., Kellogg, T.B., 1979. Recent benthic foraminiferal distribution from the Ross Sea, Antarctica: relation to ecologic and oceanographic conditions. Journal of Foraminiferal Research 9, 250–269.

Pisias, N.G., Martinson, D.G., Moore, T.C., Shackleton, N.J., Prell, W.L., Hays, J.D., Boden, G., 1984. High resolution stratigraphic correlation of benthic oxygen isotopic records spanning the last 300,000 yrs. Marine Geology 56, 119–136.

Salvi, C., Salvi, G., Brambati, A., 2000. Paleoenvironmental characteristics in core ANTA96 5 bis (Glomar Challenger Basin-Ross Sea-Antarctica). In: Brambati, A. (Ed.), Proceedings of the Workshop "Paleoclimatic Reconstructions from Marine Sediments of the Ross Sea (Antarctica) and Southern Ocean", Terra Antarctica Reports, vol. 4, pp. 179–184.

Shanmugam, G., 2000. 50 years of the turbidite paradigm (1950s–1990s): deep-water processes and facies models—a critical prospective. Marine and Petroleum Geology 17, 285–342.

Shipp, S.S., Anderson, J.B., Domack, E.W., 1999. Acoustic signature of the Late Pleistocene fluctuations of the West Antarctic ice sheet system in the Ross Sea: a new perspective: Part. 1. Geological Society of America Bulletin 111, 1486–1516.

Tolotti, R., 2002. Associazioni a diatomee polari nel mare di Ross (Antartide): ricostruzione paleoambientale e paleoclimatica. Ph.D. Thesis, Università degli Studi di Trieste, Italy.

Wentworth, C.K., 1922. A scale of grade and class terms for clastic sediments. Journal of Geology 30, 377–392.